ELSEVIER

International Journal of Mass Spectrometry 212 (2001) 455–466

International Journal of Mass Spectrometry

www.elsevier.com/locate/ijms

Examination of barriered and barrierless hydrogen atom abstraction reactions by organic radical cations: the cytosine radical cation

Jason M. Price, Christopher J. Petzold, H.C. Michelle Byrd, Hilkka I. Kenttämaa*

Department of Chemistry, Purdue University, West Lafayette, IN 47907-1393, USA

Received 27 April 2001; accepted 31 July 2001

Abstract

The radical cations of the nucleobases cytosine and adenine are easily generated in a dual cell Fourier transform ion cyclotron resonance mass spectrometer by using the technique of laser-induced acoustic desorption coupled with electron ionization. The cytosine radical cation is found to undergo facile hydrogen atom abstraction reactions with a variety of neutral reagents even when barrierless, exothermic electron transfer reactions are expected to dominate. In contrast, the adenine radical cation undergoes hydrogen atom abstraction only slowly in most of the cases studied. The ionic curve-crossing model is used to rationalize these results. Some of the thermodynamic and molecular properties of a radical cation that are favorable for efficient hydrogen atom abstraction are described in this article. Based on this analysis, dimethyl sulfoxide radical cation was predicted to abstract hydrogen atoms efficiently. Indeed, it was found to abstract hydrogen atoms at rates similar to cytosine radical cation. The transition from barriered to barrierless hydrogen atom abstraction that occurs as the ionization energy of the neutral hydrogen atom donor is lowered was used to "bracket" the recombination energy of cytosine radical cation at 8.9 ± 0.2 eV. (Int J Mass Spectrom 212 (2001) 455–466) © 2001 Elsevier Science B.V.

Keywords: Nucleobase radical cations; Hydrogen abstraction; FT-ICR; Ion-molecule reactions; Polar effects; Recombination energy; cytosine radical cation

1. Introduction

Radical cations of organic molecules are gaining new interest because they are important intermediates in processes leading to damage and cleavage of DNA [1] and are becoming increasingly useful in organic synthesis [2]. For example, reagents with suitable oxidation potentials can be used to generate selectively alkene radical cations that efficiently undergo cycloaddition [3], epoxidation [4], and hydrogenation reactions [5]. In the case of DNA damage, one-electron oxidation (e.g. by ultraviolet radiation of DNA) is known to generate nucleobase radical cations that either directly or indirectly induce DNA damage. A significant effort has been devoted to understanding the mechanism and kinetics of hole migration through the base pairs of the DNA strand [6–9]. Electron transfer in DNA may be stopped by separation of the hole and radical by rapid proton transfer between the bases [10]. The understanding of this and related

* Corresponding author. E-mail: hikka@purdue.edu

Dedicated to R. Graham Cooks on the occasion of his sixtieth birthday.

PII S1387-3806(01)00514-0

processes would be facilitated by better knowledge on the thermochemistry of the DNA nucleobases, including the proton affinities of the neutral bases as well as the recombination energies and acidities of the radical cations.

The thermochemical values relating to the nucleobase radical cations are not well known [11]. To this end, our research group has utilized the technique of Fourier-transform ion cyclotron resonance (FT-ICR) mass spectrometry to bracket the recombination energy (RE) and gas-phase acidity of adenine radical cation [12] and thymine radical cation [13]. Mass spectrometry is an ideal technique to measure thermochemical values and study the intrinsic (solvent-free) reactivity of radical cations. Radical cations are typically readily generated by simple electron ionization. The trapped-ion nature of the FT-ICR experiment permits ions to be stored for long periods of time, which allows them to approach thermal equilibrium through collisions with neutral molecules and emission of infrared photons [14].

In a fashion analogous to that employed in the investigations of adenine and thymine, we attempted to bracket the recombination energy of cytosine radical cation. However, this radical cation was observed to undergo hydrogen atom abstraction from neutral reagents as the predominant reaction pathway, even when electron transfer was predicted to be exothermic. Hydrogen atom abstraction by radical cations is certainly not without precedent. Electron paramagnetic resonance spectroscopy of a γ-irradiated solution of bis(trimethylsilyl)amine in Freon 11 showed the presence of a radical formed by hydrogen atom abstraction by bis(trimethylsilyl)amine radical cation from its neutral counterpart [15]. The hole transfer promoted hydrogenation of 1,1-diphenylethene occurs by sequential hydride and hydrogen atom abstractions of the 1,1-diphenylethene radical cation from tributyltin hydride [6]. Our previous work on adenine radical cation showed that it slowly abstracts a deuterium atom from perdeuterated tetrahydrofuran [12].

In this article, we examine the origins of the facile hydrogen atom abstraction of cytosine radical cation. In addition, hydrogen atom abstraction reactions of adenine radical cation and dimethyl sulfoxide radical cation are probed to compare with the cytosine data and validate the predictions made about the thermochemical and molecular properties that facilitate hydrogen atom abstraction. The high rates of normally "barriered" hydrogen atom abstractions are rationalized by using the ionic curve-crossing model [16].

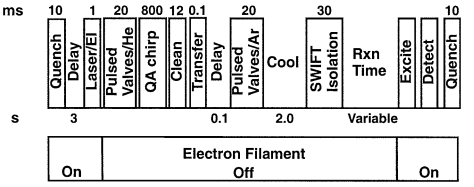

Fig. 1. Experimental sequence for the reactivity studies of nucleobase radical cations.

2. Experiment

All experiments were conducted in a dual-cell Extrel model 2001 Fourier transform ion cyclotron resonance mass spectrometer, which has been described in detail elsewhere [12]. The primary advantage of this instrument with respect to the study of ion–molecule reaction kinetics is the ability to generate and store ions in one cell and then transfer only the ion population of interest into the second cell by way of a 2 mm hole in the wall common to both cells (conductance limit). Differential pumping of the two cells significantly reduces "contamination" due to unwanted reactions of the ion population with its neutral precursor.

The general experimental sequence is shown in Fig. 1. Neutral cytosine and adenine were introduced as gas pulses into one cell of the instrument by using the technique of laser-induced acoustic desorption (LIAD) [17]. The general method of sample preparation for LIAD [18], the novel probe built to couple the LIAD technique to the FT-ICR [19], and the mechanism of desorption [18] have already been described in detail. Briefly, samples were deposited onto one side of a copper foil (10 μm thickness) by using the electrospray method. Samples of appropriate thickness were obtained by spraying approximately 10 μL

of a 10 mM solution of the nucleobase in methanol. Desorption of the neutral nucleobase was effected by a single laser shot (532 nm from a Nd:YAG laser) on the back side of the copper foil. Ionization of the nucleobases in the ion cyclotron resonance (ICR) cell was accomplished by electron ionization (70 eV for cytosine, 20 eV for adenine, 10 μA emission current) concurrent with the 1 ms laser trigger event. Depletion of the sample from an area analogous to the size of the laser pulse ($\sim 10^{-3}$ cm^2) occurred after several laser shots; consequently, multiple laser spots were used (about 12 spots per copper foil) to obtain a complete data set for analysis of reaction kinetics. Dimethyl sulfoxide (DMSO) was leaked into one cell at a nominal pressure of $3–4 \times 10^{-8}$ Torr through a variable leak valve. Ionization times and energies (200–300 ms and 12–15 eV, respectively) were optimized to maximize the signal of DMSO radical cation.

After removing all of the ions from the other cell by applying a negative potential to the remote trapping plate, the radical cations were transferred into the other cell by grounding the conductance limit for a short time (116 μs for adenine radical cation, 105 μs for cytosine radical cation, and 88 μs for DMSO radical cation). To maximize transfer efficiency, the technique of quadrupolar axialization [20] was used to refocus the ion populations' cyclotron radius along the magnetic field axis. After transfer, the ions were translationally and internally "cooled" by collisions with argon pulsed into the cell and by emission of infrared photons during the 1.5–2.5 s delay prior to isolation of the radical cations. The ion population of interest was isolated by ejecting unwanted ions from the cell by applying stored-waveform inverse Fourier transform (SWIFT) ejection pulses [21]. The isolated ions were allowed to react with a neutral reagent for a variable period of time prior to excitation and detection (see Fig. 2 for an example of a typical reaction spectrum). For each reaction time, a background correction spectrum was subtracted from the reaction spectrum to eliminate contributions from electronic noise and products arising from imperfect isolation. The background reaction spectrum was obtained by

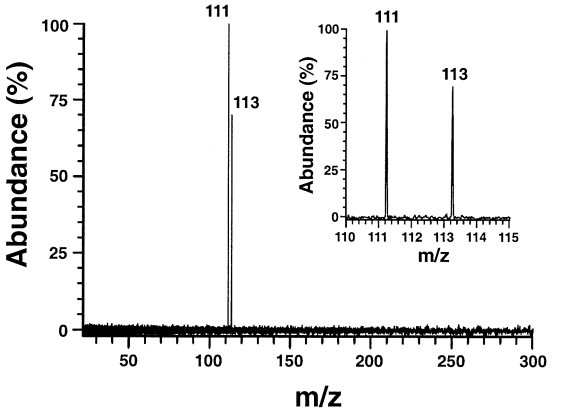

Fig. 2. Deuterium atom abstraction reaction of cytosine radical cation (*m/z* 111) with perdeuterated toluene. This reaction spectrum corresponds to a 2 s reaction time.

ejecting the reactant ion prior to reaction. The electron filament was turned off after ionization and remained off during the reaction times to ensure that the ions were near room temperature.

Because the neutral reagent was supplied at a constant pressure and its concentration was well in excess of the ion "concentration," these ion–molecule reactions follow pseudo-first-order kinetics (see Fig. 3). The negative slope of a plot of the natural logarithm of the relative ion abundance versus time gives the pseudo-first-order reaction rate constant (k'). The bimolecular rate constant (k in cm^3 molecule^{-1} s^{-1}) is obtained by dividing k' by the absolute

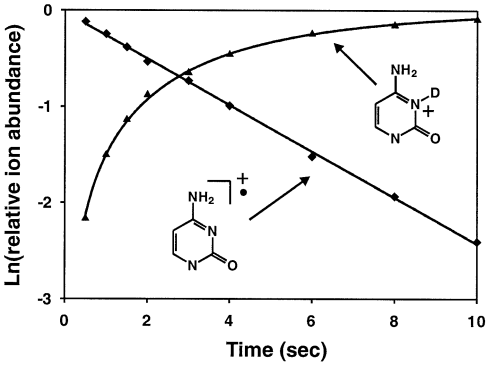

Fig. 3. Pseudo-first-order kinetic plot for the reaction of cytosine radical cation (*m/z* 111; diamonds) with perdeuterated toluene.

Table 1
Reactions of cytosine radical cation (*m/z* 111; RE 8.68 eV [29])

Neutral reagent (MW)	IE[a] (eV)	Rxn eff. (k/k_{coll})	Primary products (*m/z*)	Product branching ratios
Acetone (58)	9.703	0.05	H atom abstraction (112)	1.0
Tetrahydrofuran (72)	9.40	0.72	H atom abstraction (112)	1.0
Benzene (78)	9.244	Slow[b]	H atom abstraction (112)	1.0
Cyclohexanone (98)	9.16	0.73	H atom abstraction (112)	1.0
Toluene (92)	8.828	0.86	H atom abstraction (112)	1.0
Toluene-d_8 (100)	8.828	0.79	D atom abstraction (113)	1.0
Dimethyl sulfide (62)	8.69	1.01	H atom abstraction (112)	1.0
Ethyl methyl sulfide (76)	8.55	1.26	H atom abstraction (112)	1.0
1,3,5-Trimethylbenzene (120)	8.4	1.15	H atom abstraction (112)	0.82
			Electron transfer (120)	0.18

[a]Adiabatic ionization (IE) and recombination energies (RE) from [11].
[b]Reaction efficiencies under 0.001 cannot be measured accurately.

pressure of the neutral reagent. Correction factors to compensate for the difference between the reagent pressure measured by the ion gauge and the absolute pressure in the cell were obtained by examining ion–molecule reactions with a known rate constant. Typically, exothermic electron transfer reactions are used and are assumed to proceed at the collision rate between the ion and neutral reagent. Theoretical collision rates (k_{coll}) are obtained by using a parameterized trajectory theory [22]. Reaction efficiencies reported in this article are obtained by dividing the bimolecular reaction rate by the theoretical collision rate (k/k_{coll}).

All density functional theory (DFT) calculations were performed with the GAUSSIAN 98 suite of programs [23]. Geometries were optimized at the (U)B3LYP/6-31+G(*d*) level of theory. Frequency calculations were also performed to account for zero-point energy differences and to confirm optimized structures as minima. For the curve-crossing diagrams, the energies of the lowest energy excited ionic states corresponding to a vertical electron transfer from the neutral species to the charged species were calculated by performing single-point calculations on the optimized structures at the same level of theory using tight convergence criteria for the self-consistent field (SCF) procedure.

3. Results and discussion

The radical cation of cytosine was generated by electron ionization in one side of a dual-cell reaction chamber of a FTICR, transferred into the other cell and allowed to react with various neutral reagents. The results of these reactions are summarized in Table 1. A quick survey of the data reveals that the dominant (and often exclusive) product is formed by way of a net hydrogen atom abstraction even when electron transfer to the radical cation is exothermic. For example, cytosine radical cation reacts with 1,3,5-trimethylbenzene by hydrogen atom abstraction (82% of the primary product branching ratio) even though electron transfer is predicted to be exothermic by approximately 8 kcal/mol. The electron transfer pathway would be expected to dominate because exothermic electron transfer has been found to commonly occur at the theoretical collision rate in the gas phase [24].

One possible explanation for the unexpected absence of electron transfer products is that the observed reactivity arises from a tautomeric form of cytosine radical cation that has a lower recombination energy than that assumed for the biologically important oxo-amino tautomer of cytosine (C, Scheme 1). In fact, high-level ab initio calculations [25,26] indicate

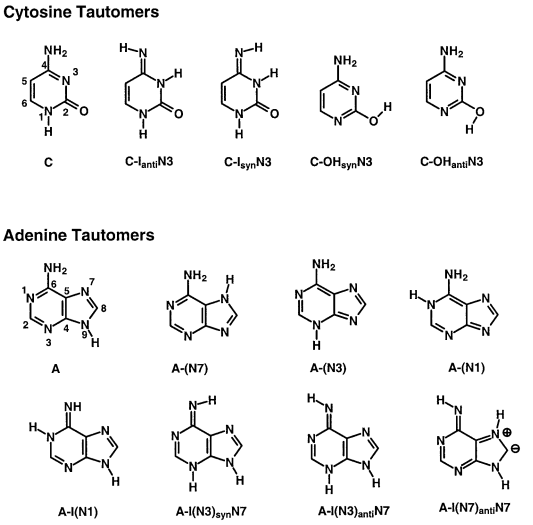

Scheme 1.

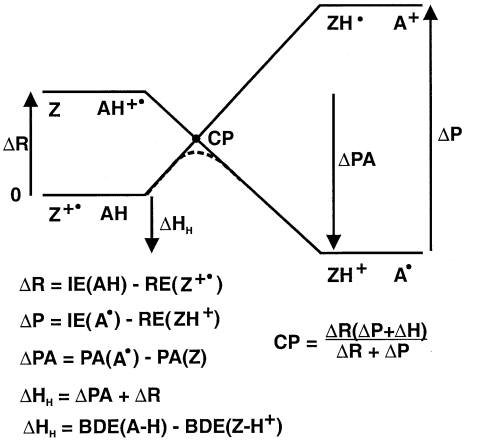

Fig. 4. Generalized ionic curve-crossing diagram for barriered hydrogen atom abstraction.

that neutral gas-phase cytosine is probably a mixture of the hydroxy-amino tautomers C–OH$_{anti}$N3 and C–OH$_{syn}$N3 and the oxo-amino tautomer C (see Scheme 1 and Table 2). Our DFT calculations indicate that the radical cation of tautomer C is <1 kcal/mol more stable than the radical cations of C–OH$_{anti}$N3 and C–OH$_{syn}$N3. However, the calculated recombination energies of all the cytosine radical cation tautomers shown in Scheme 1 are within 0.07 eV. Although it is possible that the cytosine radical cation population is a mixture of tautomers, this does not explain why the electron transfer reaction is not favored over hydrogen atom abstraction.

The results summarized in Table 1 also show that, in general, cytosine radical cation abstracts a hydrogen atom more rapidly from reagents with low ionization energies. This observation is consistent with the work of Donahue et al. who have shown that the reaction barrier for atom-transfer reactions between simple radicals correlates directly to the avoided curve crossing of the ground state and an ionic excited state [16]. A generalized curve-crossing diagram of this type is shown in Fig. 4 for hydrogen atom abstractions by radical cations. It should be noted that in the case of radical cation reactions, both the ground and excited state surfaces are ionic and that ΔR and ΔH are generally readily estimated from available thermochemical data. The energy gap between the reactant ground and excited states (ΔR) can be estimated by the difference in the recombination energy of the radical cation ($Z^{+\cdot}$) and the ionization energy

Table 2
Calculated relative energies (kcal/mol) of neutral cytosine tautomers and their radical cations

Tautomer	Neutral cytosine CCSD(T)[a]	Neutral cytosine MP4(SDTQ)[b]	Neutral cytosine B3LYP[c]	Radical cation B3LYP[c]
C	1.25	0.2	−1.88	0.0
C–OH$_{syn}$N3	0.65		0.78	0.9
C–OH$_{anti}$N3	0.00	0.0	0.0	0.4
CI–$_{syn}$N3	3.37		2.34	2.5
CI–$_{anti}$N3	1.99	2.1	0.58	1.4

[a]See [25]—CCSD(T)/cc-pVTZ//MP2/cc-pVTZ + ZPVE.
[b]See [26]—MP4(SDTQ)/6-31+G(*d*,*p*)//MP2/6-31+G(*d*,*p*).
[c]Present work—B3LYP/6-31+G(*d*) + ZPVE.

Table 3
Reactions of adenine radical cation (*m/z* 135; RE 8.55 eV [12])

Neutral reagent (MW)	IE[a] (eV)	Rxn eff. (k/k_{coll})	Primary products (*m/z*)	Branching ratios
Acetone (58)	9.703	Slow[b]	H atom abstraction (136)	1.0
Tetrahydrofuran (72)	9.40	0.016	H atom abstraction (136)	1.0
Tetrahydrofuran-d_8 (80)	9.40	0.004[c]	D atom abstraction (137)	1.0
Cyclohexanone (98)	9.16	0.004	H atom abstraction (136)	0.7
			Adduct (233)	0.3
Toluene (92)	8.828	0.002	H atom abstraction (136)	1.0
Dimethyl sulfide (62)	8.69	0.434	H atom abstraction (136)	1.0
Ethyl methyl sulfide (76)	8.55	1.06	H atom abstraction[d] (136)	1.0
1,3,5-Trimethylbenzene (120)	8.4	0.86	H atom abstraction (136)	0.95
			Electron transfer (120)	0.05

[a]Adiabatic ionization and recombination energies from [11].
[b]Reaction efficiencies under 0.001 cannot be measured accurately.
[c]From [12].
[d]This product was not reported in [12] because it was misinterpreted as resulting from reaction with neutral adenine diffusing from the other cell.

of the hydrogen atom donor (AH). The overall reaction exothermicity for hydrogen atom abstraction (ΔH_H) may be calculated either from the difference in homolytic bond dissociation energies of A–H and $Z–H^+$ or from the difference in proton affinities of Z and $A^{\cdot}$ and the relation of ΔH_H to ΔR (see Fig. 4).

Based on Fig. 4, one can envision many different qualitative "curve-crossing" diagrams simply by changing the values of ΔR, ΔP, and ΔH_H. In practice, the values may be altered by selecting reagents with the appropriate thermochemistry. We chose to examine the hydrogen atom abstraction reactions of adenine and dimethyl sulfoxide radical cations in order to study the different curve-crossing scenarios and to place the cytosine radical cation data into perspective. The former reagent is particularly attractive because it is the radical cation of a nucleobase and we have previously measured its recombination energy [12]. In addition, both theoretical [27] and experimental [28] evidence support the expectation that neutral gas-phase adenine has no low energy tautomers. Our UB3LYP/6-31+G(*d*) calculations on the radical cations of the adenine tautomers shown in Scheme 1 suggest that the radical cation of A is the lowest in energy by over 4 kcal/mol. Dimethyl sulfoxide radical cation was chosen for this study as a representative of a very different compound type with thermochemical and molecular properties that we predict to be conducive to hydrogen atom abstraction. The results of the examinations of the reactions of adenine and dimethyl sulfoxide radical cations are summarized in Tables 3 and 4, respectively.

3.1. Hydrogen atom abstraction with a barrier

The general curve-crossing diagram shown in Fig. 4 depicts a typical case where hydrogen atom abstraction involves overcoming an energy barrier. Such a barrier will exist when electron transfer to the radical cation from the hydrogen atom donor is endothermic (i.e. when the adiabatic ionization energy of A–H > adiabatic recombination energy of $Z^{+\cdot}$). The dashed line in Tables 1, 3, and 4 shows the point at which the transition from endothermic electron transfer to exothermic electron transfer is predicted to occur. Above this dashed line, the electron transfer reaction is endothermic and reaction efficiencies for hydrogen atom abstraction vary from no reaction (large barrier) to near collision rate (small barrier). The only product observed for these "barriered" reactions arises from a net hydrogen atom abstraction, with the exception of the reaction of adenine radical cation with cyclohex-

Table 4
Reactions of dimethyl sulfoxide radical cation (*m/z* 78; RE[a] 9.1 eV)

Neutral reagent (MW)	IE[a] (eV)	Rxn eff. (k/k_{coll})	Primary products (*m/z*)	Branching ratios
Ethanol (46)	10.48	0.13	H atom abstraction (79)	1.0
Diethyl ether (74)	9.51	0.75	H atom abstraction (79)	1.0
Tetrahydrofuran (72)	9.40	0.76	H atom abstraction (79)	1.0
Benzene-d_6 (84)	9.244		No reaction	
Toluene (92)	8.828	0.98	H atom abstraction (79)	0.97
			Electron transfer (92)	0.03
Toluene-d_8 (100)	8.828	0.99	D atom abstraction (80)	0.92
			H atom abstraction (79)[b]	0.04
			Electron transfer (100)	0.04
Dimethyl sulfide (62)	8.69	1.09	H atom abstraction (79)	0.97
			Electron transfer (62)	0.03
1,3,5-Trimethylbenzene (120)	8.4	0.91	H atom abstraction (79)	0.50
			Electron transfer (120)	0.50

[a]Adiabatic ionization and recombination energies from [11], and references cited therein.
[b]H atom abstraction from the rapid hydrogen atom abstraction from neutral dimethyl sulfoxide diffusing from the other cell.

anone where an addition pathway competes. It should be noted that there is a large variation in the experimental ionization energies [29,30] reported for the nucleobases and poor agreement between theory [31,32] and experiment (see Table 5). The experimental recombination energy of 8.68 eV [29] used in Table 1 was chosen based on its agreement with second-order Møller–Plesset calculations [31].

In the ionic curve-crossing model, the height of the reaction barrier (and hence the rate of reaction) will be critically dependent on the reactant and product energy gaps (ΔR and ΔP) and the reaction exothermicity (ΔH_H) (see Fig. 4). Fig. 5 shows three computationally estimated ionic curve-crossing diagrams for the reactions of cytosine radical cation with the hydrogen atom donors acetone (1), tetrahydrofuran (2) and toluene (3). The predicted energy ordering of the barrier heights (1) > (2) > (3) agrees qualitatively with that which would be predicted based on the experimental reaction efficiencies (0.05, 0.72, and 0.86 respectively; Table 1).

Similar results are obtained for DMSO radical cation. This radical cation abstracts a hydrogen atom about five times faster from tetrahydrofuran (THF) than from ethanol (reaction efficiency of 0.68 versus 0.13; Table 4) despite the fact that the reaction exothermicity is nearly identical for both reactions. The slower reaction of DMSO radical cation with ethanol may be attributed to the larger reactant and product energy gaps (ΔR of 50 kcal/mol versus 29

Table 5
Experimental and calculated values of the adiabatic IEs of cytosine and adenine

Nucleobase	Expt[a] (eV)	Expt[b] (eV)	Expt[c] (eV)	Calc[d] (eV)	Calc[e] (eV)	Calc[f] (eV)
Cytosine	. . .	8.68	8.45	8.74	8.57	8.53
Adenine	8.55	8.26		8.18	8.09	8.06

[a]See [12]—bracketing.
[b]See [29]—photoionization mass spectrometry.
[c]See [30]—photoelectron spectroscopy.
[d]See [31]—ROMP2/6-31+G(d)//ROHF/6-31G(*d*).
[e]See [32]—B3LYP/6-311+G(2*df*,*p*).
[f]Present work—B3LYP/6-31+G(*d*).

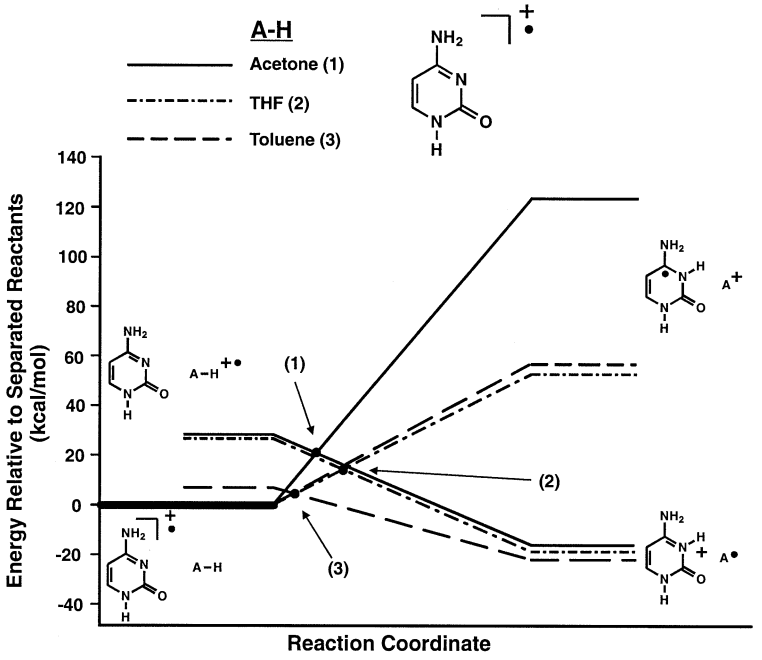

Fig. 5. Ionic curve-crossing diagrams for the reactions of cytosine radical cation with acetone (1), tetrahydrofuran (2), and toluene (3).

kcal/mol and ΔP of 70 kcal/mol versus 58 kcal/mol for the ethanol and THF reactions, respectively). DMSO radical cation does not react with perdeuterated benzene because there are no exothermic reaction channels (both ΔR and ΔH_{H} are positive).

Curve-crossing diagrams should also give insight into the relative reaction rates of the different radical cations with the same hydrogen atom donor. The curve-crossing diagrams for the reactions of (1) cytosine, (2) DMSO, and (3) adenine radical cations with THF are illustrated in Fig. 6. Based on the relative crossing points, the expected order of the barrier heights is (1) $\leq$ (2) $<$ (3). The predicted similar barrier heights for (1) and (2) are consistent with their nearly equal reaction efficiencies (0.72 and 0.76, respectively).

Although the curve-crossing diagram does predict that adenine radical cation (3) should have the slowest reaction rate, it does not appear to explain why adenine radical cation reacts extremely slowly with most of the hydrogen atom donors with large ionization energies (reaction efficiencies $<$0.02 for acetone, THF, cyclohexanone, and toluene; Table 3). Such slow reaction rates could be indicative of slightly endothermic reactions; however, this is not the case for many of the hydrogen atom abstraction reactions of adenine radical cation. For example, the reactions of adenine radical cation with THF and toluene are at least as exothermic as the dimethyl sulfide reaction (an exothermic reaction occurring at a high efficiency; Table 3). The relevant experimentally determined bond dissociation energies are 92.0, 88.5, and 92.0 kcal/mol, respectively [33]. Other factors not taken into account by the curve-crossing model appear to be important in the case of adenine radical cation and are discussed in Sec. 3.1.2.

3.1.1. Spin delocalization

The exothermicity of a hydrogen atom abstraction reaction is given by the difference in bond dissociation energies (BDEs) of the breaking and forming bonds. The BDEs of the hydrogen atom donors (A–H) used in this study are well known and the BDEs of the forming $Z–H^+$ bonds can be estimated by the use of a thermochemical cycle. For example, Scheme 2 shows that the BDE for the O–H bond in O-proto-

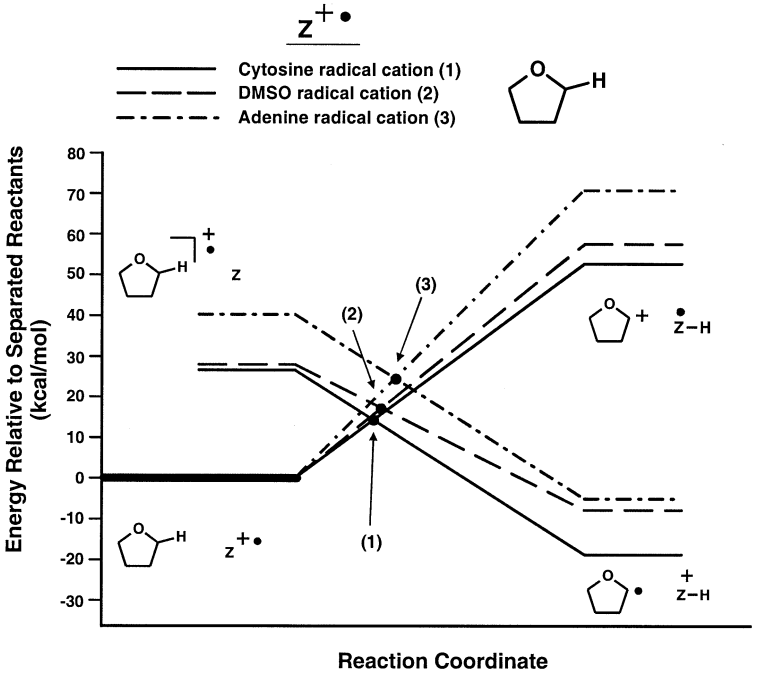

Fig. 6. Ionic curve-crossing diagrams for the reactions of cytosine (1), dimethyl sulfoxide (2), and adenine (3) radical cations with tetrahydrofuran.

nated cytosine can be calculated by subtracting the ionization energy (IE) of cytosine and the proton affinity (PA) of the cytosine O from the IE of hydrogen atom. The important general conclusion from Scheme 2 is that the largest Z–H^+ BDE (hence, the most exothermic hydrogen atom abstraction by radical cation $Z^{+\cdot}$) occurs at the site of the highest proton affinity of Z. For the oxo-amino tautomer of cytosine (C, Scheme 1), the carbonyl oxygen and N3 are calculated to have the highest (and nearly identical) proton affinities [26]. For adenine (A, Scheme 1),

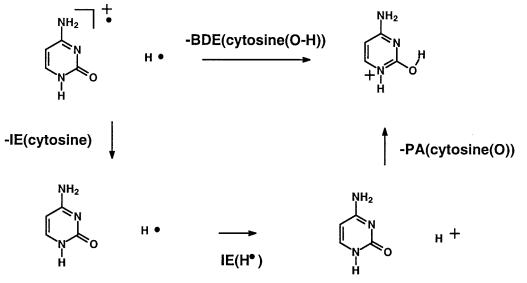

Scheme 2.

protonation at N1 is favored by 2.0 kcal/mol over protonation at N3 [26]. In the case of DMSO, protonation at oxygen is calculated to be favored by almost 29 kcal/mol over protonation at sulfur [34].

The radical cations of adenine and cytosine have both the charge and radical significantly delocalized through π orbitals. Because the barriered hydrogen atom abstractions by these radical cations are formally radical in nature, the distribution of the odd spin throughout the molecule should be important. Calculations at the UB3LYP/6-31+G(*d*) level of theory show that the odd spin (in parentheses) is localized heavily on the two most basic sites of cytosine radical cation, O2 (0.51) and N3 (0.30). In other words, the odd spin resides on the sites where the hydrogen atom abstraction reaction is most exothermic. The situation is much the same for DMSO radical cation where the odd spin largely resides on the oxygen (0.58).

For adenine radical cation, however, the odd spin is more delocalized and the largest fraction is distributed over nonbasic sites including the amino nitrogen

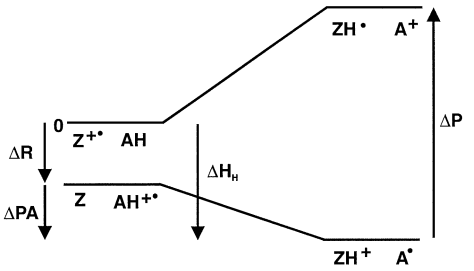

Fig. 7. Generalized ionic-curve-crossing diagram for barrierless hydrogen atom abstraction.

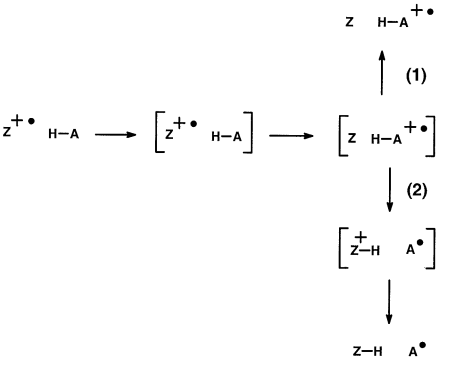

Fig. 8. Mechanism for barrierless (indirect) hydrogen atom abstraction.

(0.29), C5 (0.21), and C8 (0.20). The proton affinities of these sites relative to N1 (the most basic site in adenine) are calculated at B3LYP/6-31+G(*d*) to be 17.5, 34.7, and 31.0 kcal/mol lower, respectively. The spin density at the N1 position of adenine is calculated to be very low (0.009). Based on the calculated spin densities, the only likely site for hydrogen atom abstraction is N3 (0.20), which reduces the exothermicity for hydrogen atom abstraction by 2 kcal/mol. It is this combination of increased spin delocalization and reduced reaction exothermicity that probably leads to the unexpectedly slow hydrogen atom abstraction reactions for adenine radical cation.

3.2. Barrierless (indirect) hydrogen atom abstraction reactions

Net hydrogen atom abstraction can occur without a barrier when the adiabatic ionization energy of A–H is lower than the recombination energy of $Z^{+\cdot}$ (see Fig. 7). In this case, an exothermic (and barrierless) electron transfer can occur within the collision complex [Fig. 8, pathway (1)] to yield $A–H^{+\cdot}$ and Z. If the proton affinity of Z is greater than the acidity of $A–H^{+\cdot}$ and the collision complex is sufficiently long lived, then a proton transfer reaction will follow and ultimately result in a rapid net hydrogen atom abstraction [Fig. 8, pathway (2)].

Reactions of the radical cations with the hydrogen donors below the dashed line in Tables 1, 3, and 4 fall into this category. In every case, the reaction rates are at or very near the theoretical collision rate, as would be expected for a barrierless pathway. Because the indirect hydrogen atom abstraction occurs without a barrier, there should be no deuterium isotope effect. Indeed, dimethyl sulfoxide radical cation reacts with both toluene and perdeuterated toluene at collision rate (reaction efficiencies of 0.98 and 0.99, respectively; Table 4). This is in contrast to the barriered reactions of adenine radical cation with tetrahydrofuran and perdeuterated tetrahydrofuran where a deuterium isotope effect of about 4 is observed (reaction efficiencies of 0.016 and 0.004 respectively; Table 3).

Electron transfer products are observed only when the electron transfer is moderately exothermic (about 4 kcal/mol). As the electron transfer becomes more exothermic, the lifetime of the collision complex is likely to be shorter and the dissociation of the complex competes with the proton transfer step. This is evident in the reactions of DMSO radical cation where electron transfer accounts for 3% of the branching ratio in its reaction with dimethyl sulfide (exothermicity of about 9 kcal/mol) and 50% of the branching ratio with 1,3,5-trimethylbenzene (exothermicity of 16 kcal/mol).

The barrierless hydrogen atom abstraction by cytosine radical cation masks electron transfer products and makes bracketing the recombination energy difficult. One may assume that the transition from barriered to barrierless hydrogen atom abstraction occurs near the adiabatic recombination energy of the radical cation. Adenine radical cation provides a good test case for this assumption because its recombination energy is known to be 8.55 ± 0.1 eV [12]. The

hydrogen atom transfer reaction between adenine radical cation and dimethyl sulfide (IE = 8.69 eV) must have a barrier because its efficiency is only 0.43 whereas the reaction with ethyl methyl sulfide (IE = 8.55 eV) is barrierless (reaction efficiency of 1.06). Based on the hydrogen atom abstraction efficiencies, the recombinant energy (RE) of adenine radical cation is concluded to be 8.62 ± 0.1 eV, which is consistent with the bracketed value. Obtaining a good value for the RE of cytosine radical cation is more difficult because the reaction efficiencies decrease only very slowly from collision rate as the ionization energies of the neutral reagents increase. Toluene (IE = 8.828 eV) provides an unsatisfying bracket point because the reaction efficiency with this reagent is very near the collision rate and no deuterium isotope effect was observed within the error of the experiment (efficiencies of 0.86 and 0.79 for the undeuterated and deuterated toluene, respectively). Clearly, the RE of cytosine radical cation is less than 9.2 eV because no electron transfer was observed in its extremely slow reaction with benzene. Cytosine radical cation reacts at the theoretical collision rate with dimethyl sulfide (IE = 8.69 eV) but only at 73% of the collision rate with cyclohexanone (IE = 9.16 eV). For comparison, DMSO radical cation (RE = 9.1 eV) reacts at similar rates with reagents with IEs several tenths of an electron volt higher (e.g. THF and diethyl ether in Table 4). The RE of cytosine radical cation is therefore estimated to be 8.9 ± 0.2 eV.

4. Conclusions

In this manuscript we show that the properties of a radical cation ($Z^{+\cdot}$) that are conducive to efficient hydrogen abstraction include: a high recombination energy; a large proton affinity for its neutral analog (Z); a large spin density at the atom in $Z^{+\cdot}$ that has the largest proton affinity in Z; a large proton affinity for its conjugate base $Z^{\cdot}$ to eliminate a competing pathway involving proton transfer from $Z^{+\cdot}$ to the neutral reagent.

Cytosine radical cation has all four of these properties. Therefore, it abstracts a hydrogen atom efficiently from a wide variety of hydrogen atom donors, including tetrahydrofuran, a model of the sugar moiety of DNA. Cytosine radical cation abstracts a hydrogen atom at collision rate when the ionization energy of the hydrogen atom donor is ~8.8 eV and below. Based on these rate data, the recombination energy of cytosine is estimated to be 8.9 ± 0.2 eV.

Acknowledgements

This article is dedicated to Graham Cooks. Without him, one of the authors (H.I.K.) would never have left Finland and experienced the wonders of a happy marriage and power of FT-ICR mass spectrometry. The authors would like to thank the Jonathan Amy Facility for Chemical Instrumentation (JAFC) and especially Mark Carlsen, without whose expertise in troubleshooting and repairing the aging electronics of the Extrel 2001 FT-ICR, these experiments may have had to be carried out at atmospheric pressure. The authors also thank the NIH for funding this work.

References

[1] C.J. Burrows, J.G. Muller, Chem. Rev. 98 (1998) 1109.
[2] N.L. Bauld, Advances in Electron Transfer Chemistry, Vol. 2, P.S. Mariano (Ed.), JAI Press, Greenwich, CT, 1992, p. 1.
[3] N.L. Bauld, Tetrahedron 45 (1989) 5307.
[4] N.L. Bauld, G.A. Mirafzal, J. Am. Chem. Soc. 113 (1991) 3613.
[5] G.A. Mirafzal, J. Liu, N.L. Bauld, J. Am. Chem. Soc. 115 (1993) 6072.
[6] G.B. Schuster, Acc. Chem. Res. 33 (2000) 253.
[7] M. Bixon, J. Jortner, J. Phys. Chem. B 104 (2000) 3906.
[8] F.D. Lewis, R.L. Letsinger, M.R. Wasielewski, Acc. Chem. Res. 34 (2001) 159.
[9] B. Giese, Acc. Chem. Res. 33 (2000) 631.
[10] S. Steenken, Biol. Chem. 378 (1997) 1293.
[11] S.G. Lias, Ionization Energy Evaluation, NIST Standards Reference Database Number 69, W.G. Mallard, P.J. Linstrom (Eds.), February 2000, National Institute of Standards and Technology, Gaithersburg, MD, 20899 (http://webbook.nist.gov).
[12] C.T. Hwang, C.L. Stumpf, Y.Q. Yu, H.I. Kenttämaa, Int. J. Mass Spectrom. 182/183 (1999) 253.
[13] C.L. Stumpf, L.E. Ramirez-Arízmendi, C.J. Petzold, J.M. Price, H.I. Kenttämaa, unpublished.
[14] R.C. Dunbar, Mass. Spectrom. Rev. 11 (1992) 309.
[15] C.J. Rhodes, J. Chem. Soc. Perkin Trans. 2 (1992) 235.

[16] N.M. Donahue, J.S. Clarke, J.G. Anderson, J. Phys. Chem. A 102 (1998) 3923.
[17] B. Lindner. Int. J. Mass Spectrom. Ion Processes 103 (1991) 203.
[18] J. Pérez, L.E. Ramirez-Arízmendi, C.J. Petzold, L.P. Guler, E.D. Nelson, H.I. Kenttämaa, Int. J. Mass Spectrom. 198 (2000) 173.
[19] J. Pérez, C.J. Petzold, M.A. Watkins, W.E. Vaughn, H.I. Kenttämaa, J. Am. Soc. Mass Spectrom. 10 (1999) 1105.
[20] L. Schweikhard, S. Guan, A.G. Marshall, Int. J. Mass Spectrom. Ion Processes 120 (1992) 71.
[21] A.G. Marshall, T.C. Wang, T.L. Ricca, J. Am. Chem. Soc. 107 (1985) 7893.
[22] T. Su, W.J. Chesnavich, J. Chem. Phys. 76 (1982) 5183.
[23] GAUSSIAN 98(Revision A.7), M.J. Frisch, G.W. Trucks, H.B. Schlegel, G.E. Scuseria, M.A. Robb, J.R. Cheeseman, V.G. Zakrzewski, J.A. Montgomery, R.E. Stratmann, J.C. Burant, S. Dapprich, J.M. Millam, A.D. Daniels, K.N. Kudin, M.C. Strain, O. Farkas, J. Tomasi, V. Barone, M. Cossi, R. Cammi, B. Mennucci, C. Pomelli, C. Adamo, S. Clifford, J. Ochterski, G.A. Petersson, P.Y. Ayala, Q. Cui, K. Morokuma, D.K. Malick, A.D. Rabuck, K. Raghavachari, J.B. Foresman, J. Cioslowski, J.V. Ortiz, B.B. Stefanov, G. Liu, A. Liashenko, P. Piskorz, I. Komaromi, R. Gomperts, R.L. Martin, D.J. Fox, T. Keith, M.A. Al-Laham, C.Y. Peng, A. Nanayakkara, C. Gonzalez, M. Challacombe, P.M.W. Gill, B.G. Johnson, W. Chen, M.W. Wong, J.L. Andres, M. Head-Gordon, E.S. Replogle, J.A. Pople, Gaussian, Inc., Pittsburgh, PA, 1998.
[24] C.-C. Han, J.L. Wilbur, J.I. Brauman, J. Am. Chem. Soc. 114 (1992) 887.
[25] R. Kobayashi, J. Phys. Chem. A 102 (1998) 10813.
[26] Y. Podolyan, L. Gorb, J. Leszczynski, J. Phys. Chem. A 104 (2000) 7346.
[27] T.-K. Ha, M.J. Keller, R. Gunde, H.H. Gunthard, J. Mol. Struct. (Theochem) 364 (1996) 161.
[28] R.D. Brown, P.D. Godfrey, D. McNaughton, A.P. Pierlot, Chem. Phys. Lett. 156 (1989) 61.
[29] V.M. Orlov, A.N. Smirnov, Y.M. Varshavsky, Tetrahedron Lett. 48 (1976) 4377.
[30] D. Dougherty, E.S. Younathan, R. Voll, S. Abdulnur, S.P. McGlynn, J. Electron Spectrosc. Relat. Phenom. 13 (1978) 379.
[31] M.D. Sevilla, B. Besler, A.-O. Colson, J. Phys. Chem. 99 (1995) 1060.
[32] S.D. Wetmore, R.J. Boyd, L.A. Eriksson, Chem. Phys. Lett. 322 (2000) 129.
[33] CRC Handbook of Chemistry and Physics 78th ed., D. R. Lide (Ed.). CRC Press, Boca Raton, FL, 1997.
[34] F. Tureček, J. Phys. Chem. A 102 (1998) 4703.